CERN-TH.5979/91
BI-TP 91/01

Testing the Local $SU(2)_L \times U(1)_Y$ Symmetry of Vector-Boson-Fermion Interactions †*

J.-L. Kneur, M. Kuroda **

Fakultät für Physik
Universität Bielefeld
D-4800 Bielefeld 1
Germany

and

D. Schildknecht

CERN - Theory Division
and
Fakultät für Physik
Universität Bielefeld

Abstract

One-loop corrected predictions following from the standard $SU(2)_L \times U(1)_Y$ theory, as well as predictions from an alternative which allows for local $SU(2)_L \times U(1)_Y$ violation, are confronted with the experimental data on the vector-boson masses and the electroweak mixing angle $\bar{s}_W^2(M_Z^2)$.

† In memoriam J. J. Sakurai (1933-1982), a friend and a mentor of one of the present authors (D. S.)

* Supported by the Minister for Research and Technology (BMFT) of the Federal Republic of Germany.

** Permanent address: Department of Physics, Meiji-Gakuin-University, Yokohama, Japan.

CERN-TH.5979/91
BI-TP 91/01
January 1991

The purpose of the present note is twofold:

i) To present the one-loop corrected predictions of the $SU(2)_L \times U(1)_Y$ electroweak theory[1] in their most informative and economic form by plotting the predictions for the $W^\pm$ mass, M_W, against the electroweak mixing angle at the Z^0 mass shell, $\bar{s}^2_W$, using the Higgs mass, m_H, and the mass of the top quark, m_t, as free parameters, in order to subsequently compare the predictions for M_W and $\bar{s}^2_W$ with the experimental data.

ii) To quantify how well the local $SU(2)_L \times U(1)_Y$ symmetry of vector-boson-fermion interactions underlying the standard electroweak theory is actually tested by electroweak precision data at the Z^0 peak. For this purpose, the empirical data will be compared with the predictions of an alternative theory which allows for $SU(2)_L \times U(1)_Y$ breaking terms and contains the standard theory as a limiting case. We will start our treatment with item i) and subsequently turn to item ii).

The radiative corrections to the $SU(2)_L \times U(1)_Y$ electroweak theory are most conveniently taken into account by introducing scale-dependent ("running") parameters,[2,3,4] in particular, running coupling constants and running masses. The universal † Fermi coupling, G_F, in one-loop order is then represented by (compare (4.3) in ref. 3)

$$4\sqrt{2}G_F = \frac{e^2(M_Z^2)}{M_Z^2\, \bar{s}^2_W(1-\bar{s}^2_W)}\, \frac{1}{\bar{\rho}(M_Z^2)}\, \left(1-\delta(M_Z^2)\right) . \tag{1}$$

In (1), $\bar{s}^2_W$ refers to the running weak mixing angle evaluated at the scale M_Z^2, i.e., $\bar{s}^2_W \equiv \bar{s}^2_W(M_Z^2)$. The running electromagnetic coupling constant at the scale M_Z^2 in (1) is given by

$$e^2(M_Z^2) = \frac{e^2(0)}{1-e^2(0)\left(\delta_{QQ}(0)-\delta_{QQ}(M_Z^2)\right)}, \tag{2}$$

where the function $\delta_{QQ}(q^2)$ contains the (dominant) vacuum-polarization corrections to the photon propagator due to fermion loops and the genuine †† [3] vacuum polarization due to vector bosons. For the explicit expression for $\delta_{QQ}(q^2)$ and similar functions to be introduced below, we refer to ref. 3. We note the numerical result, however, of

$$\frac{e^2(M_Z^2)}{4\pi} = \alpha(M_Z^2) \cong \frac{1}{128.8} \tag{3}$$

which will be useful for the ensuing numerical discussions. The small additional correction $\delta(M_Z^2)$ in (1) is given by

$$\delta(M_Z^2) = \frac{e^2(0)}{\bar{s}^2_W(M_Z^2)}\left(\delta_\pm(M_Z^2)-\delta_{Q3}(M_Z^2)\right), \tag{4}$$

† The "universal" Fermi coupling is defined [3] by the $q^2 \to 0$ limit of the dressed $W^\pm$-propagator.

†† The "genuine" vacuum polarization due to vector bosons, because of gauge-invariance reasons, contains contributions from vacuum polarization-diagrams as well as from vertex- and box-diagrams.

where $\delta_\pm(q^2)$ and $\delta_{Q3}(q^2)$ originate from vacuum-polarization corrections to the $W^\pm$ and Z° propagators, respectively. Physically the quantity $\delta(M_Z^2)$ describes the correction to the Born-term relation between $\bar{s}^2_W$ and the electromagnetic and weak couplings,

$$\bar{s}^2_W = \frac{e^2(M_Z^2)}{g^2_W(M_Z^2)}\left(1-\delta(M_Z^2)\right). \tag{5}$$

An approximate expression for $\delta(M_Z^2)$ will be given below. Finally, $\bar{\rho}(M_Z^2)$ in (1) describes the amount of global $SU(2)$ violation † induced by radiative effects, in particular, by the large mass of the top quark, $m_t > M_W$. It is defined in terms of running masses by

$$\bar{\rho}(q^2) \equiv \frac{M_W^2(q^2)}{M_Z^2(q^2)\,\bar{c}^2_W(q^2)}. \tag{6}$$

For the explicit expression for $\bar{\rho}(q^2)$ we again refer to ref. 3. An approximate expression for $\bar{\rho}$ will be given below. Specializing (6) to $q^2 = M_Z^2$, and expressing $M_W^2(M_Z^2)$ in terms of the physical $W^\pm$ mass, $M_W(M_W^2)$, we obtain the radiatively corrected tree-level relation between the $W^\pm$ and Z° masses,

$$M_W^2 = \bar{\rho}(M_Z^2)\, M_Z^2\,(1-\bar{s}^2_W)\left(1-\frac{e^2(0)}{\bar{s}^2_W}\left(\delta_\pm(M_W^2)-\delta_\pm(M_Z^2)\right)\right), \tag{7}$$

which will be useful subsequently. The correction on the right-hand side of (7) describes the evolution of the running $W^\pm$ mass from the scale $q^2 = M_W^2$ to the scale $q^2 = M_Z^2$.

The universal Fermi coupling, G_F, in (1) is related [3] to the empirical Fermi coupling measured in $\mu^\pm$ decay by an ultraviolet-finite correction due to box and vertex diagrams, i. e.,

$$G_\mu = G_F\left(1+\epsilon_{box}+\epsilon_{vertex}\right), \tag{8}$$

where

$$\epsilon_{box}+\epsilon_{vertex} \cong 0.00755 \text{ for } \bar{s}^2_W = 0.23.$$

Upon substituting (8) into (1), and combining (1) with (7), one may now predict $\bar{s}^2_W$ and M_W in terms of the empirically known imput parameters $\alpha(0), G_\mu$ and M_Z for any pair of values chosen for m_t and m_H. An iterative procedure is to be used in the calculation, as the corrections incorporated in $\bar{\rho}(M_Z^2), \delta_\pm(M_Z^2)$, etc. are dependent on M_W and $\bar{s}^2_W$ themselves.

Using

$$\begin{aligned} \alpha(0) &= 1/137.036 \\ G_\mu &= 1{,}166389\ 10^{-5}\ (GeV)^{-2} \\ M_Z &= 91.177\ GeV\ ^{5} \end{aligned} \tag{9}$$

as input, we find the results for M_W and $\bar{s}^2_W$ which are displayed in Fig. 1a. For comparison, in Fig. 1a, we also give the empirical results for M_W and $\bar{s}^2_W$. The results [6] for M_W are

† This global $SU(2)$ symmetry refers to the so-called "custodial" $SU(2)$ which guarantees equality of the masses of the neutral and charged members of the $W^\pm W^3$ triplet in the limit in which mixing in the neutral $W^3 - B$ boson sector is turned off.

based on the mass ratio M_W/M_Z from the CDF and UA2 measurements and on M_W/M_Z extracted from neutrino scattering, both ratios being combined with the value of M_Z from LEP. The value[5] for $\bar{s}_W^2$ is the average of the results obtained by the ALEPH, DELPHI, L3 and OPAL collaborations. In Fig. 1a, we also indicate the accuracy which is expected to be obtainable at LEP ($\delta\bar{s}_W^2 \simeq \pm 0.0004$ with polarized $e^\pm$ beams[7], $\delta M_W \simeq \pm 70$ MeV at LEP200) in the future. From Fig. 1a, we draw the following conclusions:

a) Consistency of the data with the $SU(2)_L \times U(1)_Y$ predictions requires the mass of the top quark to lie between the bounds of approximately

$$100\ GeV \leq m_t \leq 200\ GeV.$$

b) Obviously, for a precision test of the $SU(2)_L \times U(1)_Y$ theory the discovery of the top quark and an accurate determination of its mass will be indispensable.

In order to further explore the significance of the comparison of M_W and $\bar{s}_W^2$ with the empirical data in Fig. 1a, we now turn to the question [2] of how far the predictions in Fig. 1a are determined by the "known" physics of the vector-boson-fermion interactions, and how far they are associated with the "new", empirically unknown physics of the $W^\pm, Z^\circ$ self-interactions and the $W^\pm, Z^\circ$-Higgs-boson interactions which enter the (genuine) bosonic vacuum-polarization contributions to the $W^\pm$ and Z° propagators. Accordingly, we put the genuine bosonic vacuum polarization to the $W^\pm$ and Z° propagators equal to zero. The functions $\delta(M_Z^2)$ and $\bar{\rho}(M_Z^2)$ in (1), (7), respectively, then only depend on m_t (i. e. they become independent of m_H). The exact dependence on m_t is complicated[2], but a considerable simplification is obtained in the limit of $m_t \gg M_W$. In this limit we have (with $\bar{c}_W^2 \equiv 1 - \bar{s}_W^2$)

$$\bar{\rho}(M_Z^2) = 1 + \frac{3\sqrt{2}}{16\pi^2} G_\mu\ m_t^2 + \frac{\sqrt{2}}{24\pi^2} G_\mu M_W^2 \frac{1}{\bar{c}_W^2}(1 + 2\bar{c}_W^2)\, ln \frac{m_t^2}{M_Z^2} \qquad (10a)$$

and

$$\delta(M_Z^2) = \frac{\sqrt{2}G_\mu}{12\pi^2} M_W^2\ ln \frac{m_t^2}{M_Z^2}. \qquad (10b)$$

In part of the ensuing numerical evaluation we will neglect the small correction in (7) which is due to the running of $M_W^2(q^2)$ between the scales $q^2 = M_W^2$ and $q^2 = M_Z^2$, i.e., we will put

$$\delta_\pm(M_W^2) - \delta_\pm(M_Z^2) = 0. \qquad (11)$$

The numerical evaluation of (1) and (7) (with (3) and (8)) is now carried out in several steps. First of all, we adopt the approximation (11) and use for $\bar{\rho}(M_Z^2)$ and $\delta(M_Z^2)$ the large- m_t approximations (10a), (10b). This yields the points marked by "o" in Fig. 1b. Secondly, we again use (11), but take into account the m_t-dependence of $\bar{\rho}(M_Z^2)$ and $\delta(M_Z^2)$ exactly [2]. This yields the points marked by "×" in Fig. 1b [†]. Finally, we drop

[†] The small discrepancy between these two evaluations vanishes for sufficiently large m_t, when the exact formulae coincide with the approximate ones given in (10a), (10b). This was also checked numerically.

the approximation (11), again using the exact m_t dependence of $\bar{\rho}(M_Z^2)$ and $\delta(M_Z^2)$. As the difference (11) is independent of m_t (for sufficiently large $m_t \gg M_W$) and (practically) only affects M_W in (7), we expect a constant vertical shift of the points marked by "×" in Fig. 1b. This is actually the case for the points marked by "⋆" in Fig. 1b.

From Fig. 1b, we conclude that the effect of the m_H-dependent (genuine) bosonic vacuum-polarization contribution to the $W^\pm, Z^\circ$ propagators is negligibly small for moderate values of $m_H \cong 100\ GeV$. The "dominant-fermion-loop approximation" [2], defined by neglecting the bosonic vacuum polarization, for moderate values of m_H practically coincides with the exact one-loop results. Assuming m_t to be known in the future, agreement of future LEP data with the predictions in Fig. 1b will allow one to conclude that the effects of the bosonic vacuum polarization are indeed small, as predicted by the $SU(2)_L \times U(1)_Y$ spontaneously broken electroweak theory. Naturally, alternatives in which the bosonic effects are suppressed by different (so far unspecified) mechanisms, can only be ruled out by the empirical verification of the gauge-theory couplings of the vector bosons and the discovery of the Higgs particle.

We turn to point ii) mentioned at the beginning of this paper, a quantification of how well high-precision data verify the local $SU(2)_L \times U(1)_Y$ symmetry postulated to hold for electroweak interactions. For this purpose, we will consider the $m_V \to \infty$ limit of a recently examined electroweak theory [8], which contains an additional vector boson triplet, $V^\pm, V^\circ$ of mass m_V. This theory actually stands for a class of several models, as various models previously considered in the literature [9,10,11] are obtained [8] from it by specialization. The Lagrangian of the extended theory in the limit of $m_V \gg M_W$ (formally to be identified with the limit $m_V \to \infty$), as far as vector-boson-fermion interactions are concerned, was found to coincide [8] with the Lagrangian proposed by Hung and Sakurai [12] on the basis of global $SU(2)$ symmetry broken by γW^3 mixing. In terms of the physical photon, $W^\pm$ and Z° fields the interaction Lagrangian of the theory for $m_V \to \infty$,

$$\begin{aligned} L_{CC} &= \frac{g_W}{\sqrt{2}}\left(W_\mu^+\ j_+^\mu + W_\mu^-\ j_-^\mu\right), \\ L_{NC} &= e\ A_\mu\ j_Q^\mu\ + g_{Z_0}\left(j_3^\mu - s_W^2 j_Q^\mu\right) Z_\mu, \end{aligned} \qquad (12)$$

looks like the $SU(2)_L \times U(1)_Y$ Lagrangian. There is an essential difference, however. In the Lagrangian (12), à la Hung and Sakurai, *four* parameters are independent in contrast to the three independent parameters of the standard $SU(2)_L \times U(1)_Y$ theory. Upon relating g_W in (12) to the Fermi coupling, G_F, via the (tree-level) relation

$$g_W^2 = 4\sqrt{2} G_F M_W^2, \qquad (13)$$

the four input parameters to be associated with (12) may be chosen as

$$(e, G_F, s_W^2, M_W). \qquad (14)$$

The Z° mass, M_Z, and the Z° coupling to fermions, g_Z, in the Hung-Sakurai model in terms of the input (14) are determined by the (tree-level) relations

$$M_Z^2 = \frac{M_W^2}{1 - s_W^4 M_W^2 \frac{4\sqrt{2}G_F}{e^2}} \qquad (15)$$

and

$$g_Z^2 = \frac{g_W^2}{1 - s_W^4 M_W^2 \frac{4\sqrt{2}G_F}{e^2}}, \tag{16}$$

respectively. These relations guarantee $\rho = 1$ at tree level. Solving (15) for M_W^2 yields M_W in terms of M_Z,

$$M_W^2 = \frac{M_Z^2}{1 + s_W^4 M_Z^2 \frac{4\sqrt{2}G_F}{e^2}}. \tag{17}$$

This relation allows us to replace the set of independent input parameters (14) by the set

$$(e, G_F, s_W^2, M_Z) \tag{18}$$

to be used subsequently. Transition to the standard $SU(2)_L \times U(1)_Y$ theory corresponds to imposing the constraint

$$s_W^2 \frac{g_W^2}{e^2} = s_W^2 \frac{4\sqrt{2}G_F M_W^2}{e^2} = 1, \tag{19}$$

which reduces the number of parameters to the canonical number of three and converts (15) and (16) to standard (tree-level) form.

For the ensuing discussion, it will be useful to quantify possible deviations from the standard $SU(2)_L \times U(1)_Y$-symmetric theory by introducing the parameter

$$\epsilon \equiv 1 - s_W^2 \frac{g_W^2}{e^2}, \tag{20}$$

which, according to (19), fulfils $\epsilon = 0$ in the $SU(2)_L \times U(1)_Y$ limit. Upon inserting (13) and (17), ϵ may be expressed in terms of the set of variables (18) via

$$\epsilon = 1 - \frac{s_W^2 \, 4\sqrt{2}G_F M_Z^2}{e^2 \left(1 + \frac{s_W^4}{e^2} 4\sqrt{2}G_F M_Z^2\right)}. \tag{21}$$

The parameter ϵ exactly quantifies the magnitude of local $SU(2)_L \times U(1)_Y$ violation contained in the Hung-Sakurai model. This is explicitly seen by going back to a representation of the interaction (12) in terms of the original fields employed before transition to the physical photon and the Z^o fields. Introducing an isovector triplet, w_μ^i, of mass M_W and mixing with the photon field, a_μ, of strength λ_W, this basic Lagrangian may be cast into the form[8] †

$$\begin{aligned} L = &-\frac{1}{4} W_{\mu\nu}^i W_i^{\mu\nu} + g_W j_i^\mu W_\mu^i + \frac{M_W^2}{2} w_\mu^i w_i^\mu \\ &+ e\left(1 - \frac{g_W \lambda_W}{e}\right) j_\mu^3 a^\mu \\ &- \frac{1}{4}\left(1 - \lambda_W^2\right) a^{\mu\nu} a_{\mu\nu} + e \, j_\mu^Y a^\mu, \end{aligned} \tag{22}$$

† Additional vector-boson photon interaction terms are suppressed in (22). They modify the trilinear and quadrilinear interactions of W, Z, γ by terms proportional to $e(1 - g_W\lambda_W/e)$ and $e^2(1 - g_W\lambda_W/e)^2$ respectively, which are neglected throughout this paper, as we concentrate on the modification of the interactions of gauge bosons with *fermions*.

where by definition

$$\begin{aligned} W_\mu^3 &= w_\mu^3 + \lambda_W \, a_\mu, \\ W_\mu^\pm &\equiv w_\mu^\pm, \end{aligned} \tag{23}$$

and where the kinetic term has non-Abelian form. Diagonalization of (22) via

$$\begin{pmatrix} a_\mu \\ w_\mu^3 \end{pmatrix} = \begin{pmatrix} 1 & \frac{-\lambda_W}{\sqrt{1-\lambda_W^2}} \\ 0 & \frac{1}{\sqrt{1-\lambda_W^2}} \end{pmatrix} \begin{pmatrix} A_\mu \\ Z_\mu \end{pmatrix} \tag{24}$$

indeed yields the fermion interaction (12), where s_W^2 is related to λ_W by

$$s_W^2 = \lambda_W \frac{e}{g_W}. \tag{25}$$

The Lagrangian (22) in the massless limit becomes invariant under local $SU(2)_L$ transformations, provided the interaction term proportional to j_μ^3 is absent. This is the case precisely for $\lambda_W = e/g_W$. The strength of the $SU(2)_L$-violating term in (22) is thus indeed determined by the parameter ϵ introduced in (20). According to (20) and (25), ϵ is given by

$$\epsilon = 1 - \frac{\lambda_W g_W}{e}, \tag{26}$$

which coincides with the coefficient of the $SU(2)_L \times U(1)_Y$-violating term in (22). We add the remark that the connection of (22) with the standard form of the $SU(2)_L \times U(1)_Y$ Lagrangian is established by introducing the field B_μ via

$$B^\mu = \sqrt{1 - \lambda_W^2} \; a^\mu. \tag{27}$$

In this notation, the Lagrangian (22) differs from the standard Lagrangian by an additional $SU(2)_L$-violating interaction term of the hypercharge field, B_μ, with the third component of the weak isovector current.

In the extended $SU(2)_L \times SU(2)_V \times U(1)_Y$ gauge theory one has [8]

$$\lambda_W g_W + \lambda_V g_V = e, \tag{28}$$

and, accordingly, the deviation of ϵ from zero is determined by the product of the γV^3 mixing strength, λ_V, and the V-boson-fermion interaction strength, g_V, via

$$\epsilon = \frac{\lambda_V g_V}{e}. \tag{29}$$

The $SU(2)_L$-breaking term in (22) thus originates from mixing with the additional heavy neutral vector boson. In a perturbative analysis of the mixing, the full (primordial) photon-fermion interaction is to be visualized as the sum of the W^3-dominance (standard) term supplemented by an additional short-range contribution of strength $\lambda_V g_V$ which originates from mixing with the "infinitely" heavy neutral member of the V-boson triplet. Compare Fig. 2.

Before presenting the predictions of the $SU(2)_L \times U(1)_Y$- violating alternative, the formulae (17) for M_W^2 and (21) for ϵ have to be radiatively corrected. The empirical data on electroweak interactions imply that the $SU(2)_L \times U(1)_Y$ predictions for the $W^\pm$ and Z^0 properties, in very good approximation at least, are actually valid. Possible mixing effects with additional heavy bosons, $V^\pm$, V^0, underlying the present analysis, must be very much suppressed. In excellent approximation, the radiative corrections (apart from terms proportional to the necessarily small mixing with the $V^\pm$, V^0 bosons) thus coincide with the standard $SU(2)_L \times U(1)_Y$ radiative corrections. Appropriately applying the radiative corrections in (1) and (7) to the expression for M_W^2 yields

$$M_W^2 = \frac{M_Z^2 \bar{\rho}\left(M_Z^2\right)\left(1 - \frac{e^2(0)}{\bar{s}_W^2}\left(\delta_\pm\left(M_W^2\right) - \delta_\pm\left(M_Z^2\right)\right)\right)}{1 + \frac{\bar{s}_W^4}{} \frac{4\sqrt{2}G_F \; M_Z^2 \; \bar{\rho}\left(M_Z^2\right)}{e^2\left(M_Z^2\right)\left(1 - \delta\left(M_Z^2\right)\right)}}. \tag{30}$$

We note in passing that the $SU(2)_L \times U(1)_Y$ formulae (1) is immediately recovered by imposing (7) as an additional constraint on (30). Likewise, ϵ in (21) is modified to

$$\epsilon(m_t) = 1 - \frac{\bar{s}_W^2}{e^2\left(M_Z^2\right)} \frac{4\sqrt{2}G_F \; M_Z^2 \bar{\rho}\left(M_Z^2\right)}{\left(1 - \delta\left(M_Z^2\right)\right)\left(1 + \frac{\bar{s}_W^4 \; 4\sqrt{2}G_F \; M_Z^2 \; \bar{\rho}\left(M_Z^2\right)}{e^2\left(M_Z^2\right)\left(1 - \delta\left(M_Z^2\right)\right)}\right)}. \tag{31}$$

Here, we have written $\epsilon(m_t)$ to indicate that the magnitude of the $SU(2)_L \times U(1)_Y$ violation corresponding to a definite value of $\bar{s}_W^2$ depends on the value of m_t†.

The predictions of the $SU(2)_L \times U(1)_Y$-violating model are presented in Fig. 3a together with the $SU(2)_L \times U(1)_Y$ predictions taken from Fig. 1 ($m_H = 100 GeV$). As expected, the local $SU(2)_L$-violation embodied in the $SU(2)_L \times U(1)_Y$-breaking alternative leads to deviations from the $SU(2)_L \times U(1)_Y$ predictions which differ from the changes in the predictions which are obtained by violating only global (custodial) $SU(2)$ symmetry via $\bar{\rho} \neq 1$ (i. e., by proceeding along the standard $SU(2)_L \times U(1)_Y$ line in the $M_W - \bar{s}_W^2$-plane of Fig. 3a). For any fixed value of m_H and m_t the $SU(2)_L \times U(1)_Y$ standard theory defines a point in the $M_W - \bar{s}_W^2$-plane of fig. 3a, while the $SU(2)_L \times U(1)_Y$-breaking alternative yields a line. The deviation from local $SU(2)_L \times U(1)_Y$ symmetry, $|\epsilon(m_t)|$, increases along the lines m_t = const with increasing distance from the standard-model points. The magnitude of $SU(2)_L \times U(1)_Y$ breaking, $\epsilon(m_t)$, allowed by the present data for M_W and $\bar{s}_W^2$, as obtained from Fig. 3a, is plotted in Fig. 3b††. This figure shows that the strength of a possible local $SU(2)_L$ violation is constrained by

$$|\epsilon(m_t)| \leq 0.016. \tag{32}$$

† Formulae (30) and (31) in principle also depend on m_H, i.e., the extended theory containing the $V^\pm$, V^0 triplet is thought to be enlarged[8,9] by a Higgs sector, or, alternatively, m_H in this context is to be understood as a logarithmic cut-off of bosonic vacuum polarization.

†† The values of $\epsilon(m_t)$ in Fig. 3b are the values of $\epsilon(m_t)$ at the intersections of the ellipse defined by the experimental errors on M_W and $\bar{s}_W^2$ with the $SU(2)_L \times U(1)_Y$-violating lines in Fig. 3a. The ellipse in Fig.3a corresponds to 68% probability.

Interpreted in terms of mixing of the photon with an additional heavy vector boson, $V^3 (m_V \gg M_W)$, according to (29), the result (32) says that a contribution of $|\epsilon| = |\lambda_V g_V / e| \leq 1.6\%$ to the saturation of e due to V^3 is allowed by present data. Alternatively, one may say that the neutral partner of the $W^\pm$, the W^3, saturates the large fraction of at least 98.4% of e. Provided m_t is known and future high-precision data agree with the standard $SU(2)_L \times U(1)_Y$ predictions, the accuracy indicated in Fig. 3a will allow one to limit $\epsilon(m_t)$ to $|\epsilon(m_t)| \leq 0.001$ approximately. Alternatively, any observed deviation from the $SU(2)_L \times U(1)_Y$ symmetry (assuming that the top-quark has been discovered) could be interpreted in terms of the existence of an additional heavy vector boson, V^3, mixed with the photon.

In summary: present data imply that vector-boson-fermion interactions fulfil a local $SU(2)_L \times U(1)_Y$ symmetry principle with high accuracy. The strength of a possible $SU(2)_L \times U(1)_Y$ -violating interaction term is constrained by $|\epsilon| e < 0.016 e$. Great progress has been made in empirically establishing the theoretically conjectured $SU(2)_L \times U(1)_Y$ electroweak symmetry by increasing the precision to which M_W is known and by the high-precision data on M_Z and $\bar{s}_W^2$. Evidently, apart from reaching higher precision on M_W and $\bar{s}_W^2$, the discovery of the top quark will be essential to establish further the validity of the $SU(2)_L \times U(1)_Y$ spontaneously broken electroweak theory. Moreover, the vector-boson self interactions of the γ, $W^\pm$ and Z^0 which follow from the postulate of local $SU(2)_L \times U(1)_Y$ symmetry have to be empirically verified, and, to literally prove the $SU(2)_L \times U(1)_Y$ theory, the existence of the Higgs particle will have to be established. Much exciting physics will be ahead of us until the nature of the electroweak interactions is fully revealed.

References

1) S. L. Glashow, Nucl. Phys. 22 (1961) 579;
S. Weinberg, Phys. Rev. Lett 19 (1967) 1264;
A. Salam, in ***Elementary particle theory***, ed. N. Svartholm, Stockholm: Almquist and Wiksell 1968 P 367.
2) G. J. Gounaris and D. Schildknecht, Z. Phys C40 (1988) 447; C42 (1989) 107.
3) M. Kuroda, G. Moultaka and D. Schildknecht, Nucl. Phys. B 350 (1991) 25.
4) D. C. Kennedy and B. W. Lynn, Nucl. Phys. B322 (1989) 1.
5) F. Dydak, Invited Talk at the International Conference on High Energy Physics, Singapore, August 1990.
6) D. Froidevaux, CERN/PPE/90-136 (1990) to appear in Proc. of the 14^{th} Internat. Conf. on Neutrino Physics and Astrophysics (Geneva 1990).
7) D. Treille, "Polarization at LEP", eds. G. Alexander et al, CERN Yellow Report 88-06 (1988) Vol.1 p.265.
8) J. L. Kneur and D. Schildknecht, CERN preprint CERN-TH. 5916/90, to appear in Nucl. Phys. B.
9) V. Barger, E. Ma and K. Whisnant, Phys. Rev. D25 (1982) 1384.
10) M. Kuroda and D. Schildknecht, Phys. Lett. 121B (1983) 173.
11) R. Casalbuoni, S. DeCurtis, D. Dominici and R. Gatto, Phys. Lett. 155B (1985) 95; Nucl. Phys. B282 (1987) 235;
G. Altarelli, R. Casalbuoni, D. Dominici, F. Feruglio and R. Gatto, Nucl. Phys. B342 (1990) 15.
12) P. Q. Hung and J. J. Sakurai, Nucl. Phys. B143 (1978) 81.

Figure Captions:

Fig. 1a Predictions of the $SU(2)_L \times U(1)_Y$ theory for M_W and $\bar{s}_W^2$ from $\alpha(0), G_\mu$ and M_Z for various values of the parameters m_t and m_H. Present data for M_W and $\bar{s}_W^2$ are indicated as well as the expected future precision of such data.

Fig. 1b The results of the dominant fermion-loop approximation (defined by omitting the m_H-dependent bosonic vacuum polarization to $W^\pm$ and Z° propagation) compared with the exact one-loop results of Fig. 1a. The points "o" and "×" use leading and full m_t dependence of $\bar{\rho}(M_Z^2)$ and $\delta(M_Z^2)$, respectively. The point "$\star$" takes into account the additional small correction $\delta_\pm(M_Z^2) - \delta_\pm(M_W^2)$ in (7). See text for details.

Fig. 2 Diagrams for γw^3 and γv^3 mixing in the limit of $m_V \to \infty$.

Fig. 3a Predictions of the $SU(2)_L \times U(1)_Y$-breaking alternative for various values of m_t. The $SU(2)_L \times U(1)_Y$ predictions are taken from Fig. 1 ($m_H = 100\ GeV$). The ellipse defines the region in the $M_W - \bar{s}_W^2$ plane which is allowed by the indicated error bars of the experimental results requiring a probability of 68% for the value of M_W and $\bar{s}_W^2$ to lie within this region.

Fig. 3b The amount of local $SU(2)_L \times U(1)_Y$ violation, $\epsilon(m_t)$, allowed by the present data for M_W and $\bar{s}_W^2$ shown in Fig. 3a.

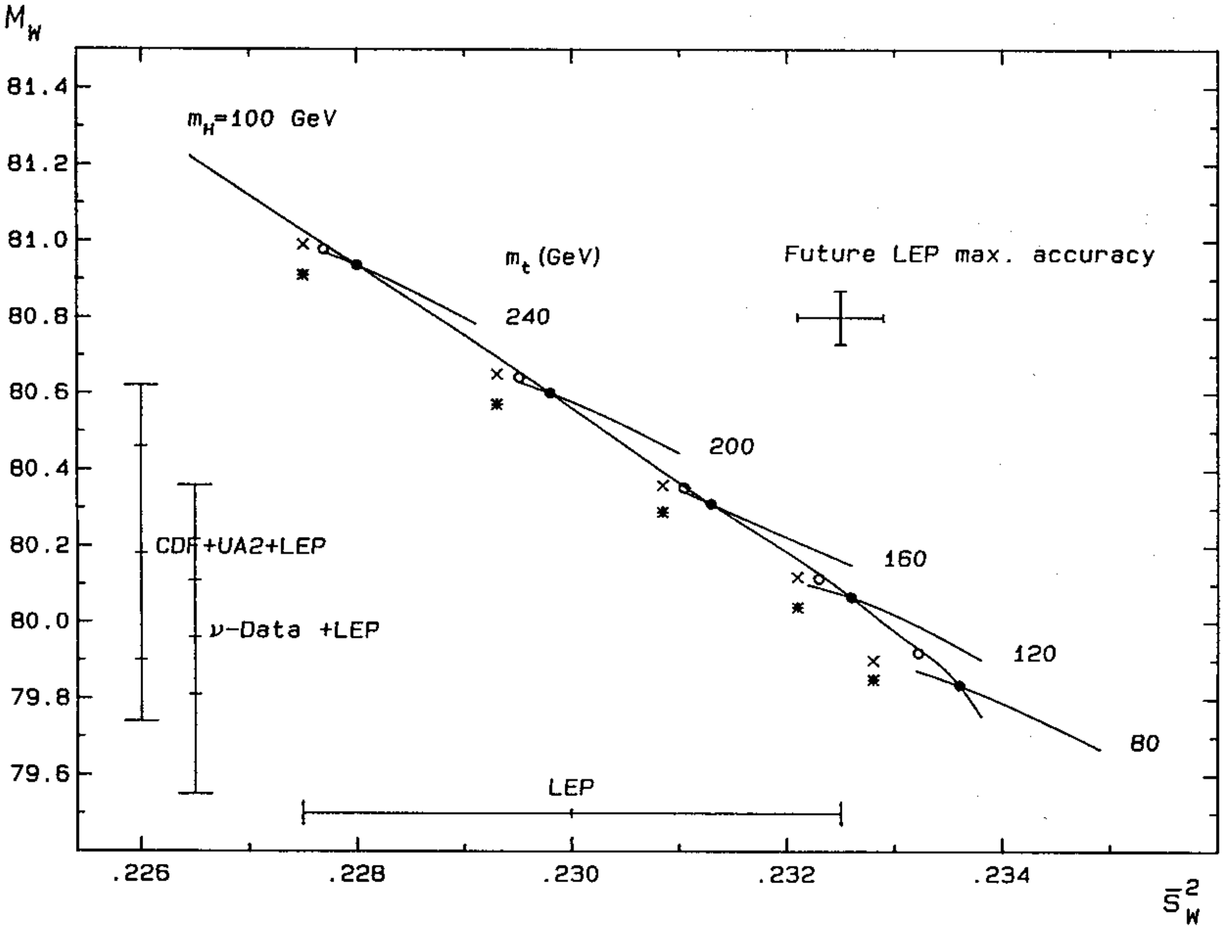

M_W
81.4
81.2
81.0
80.8
80.6
80.4
80.2
80.0
79.8
79.6
m_H=100 GeV
m_t (GeV)
240
200
160
120
80
Future LEP max. accuracy
CDF+UA2+LEP
ν-Data +LEP
LEP
.226
.228
.230
.232
.234
$\bar{s}_W^2$

Fig. 1b

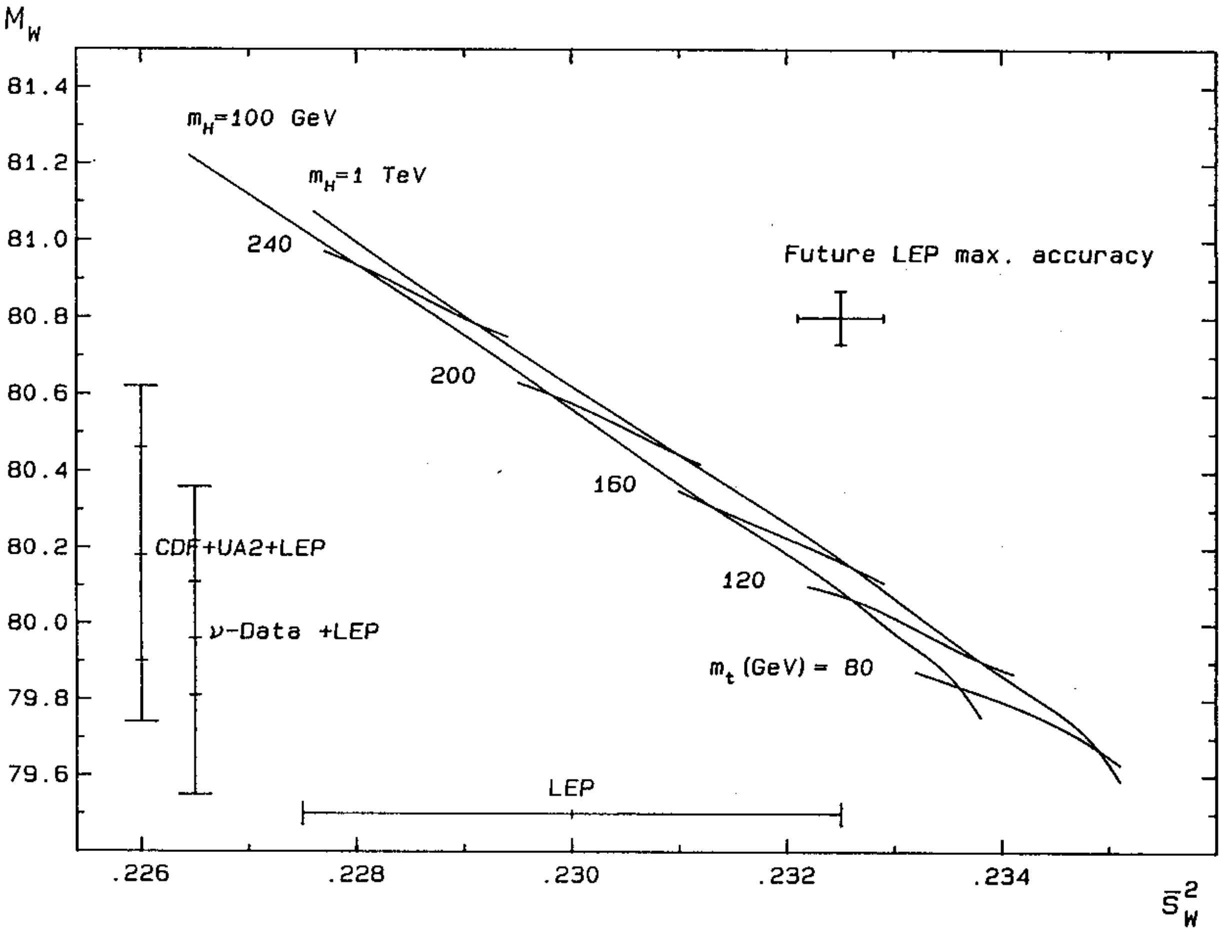

M_W
81.4
81.2
81.0
80.8
80.6
80.4
80.2
80.0
79.8
79.6
m_H=100 GeV
m_H=1 TeV
240
200
160
120
m_t (GeV) = 80
Future LEP max. accuracy
CDF+UA2+LEP
ν-Data +LEP
LEP
.226
.228
.230
.232
.234
$\bar{s}_W^2$

Fig. 1a

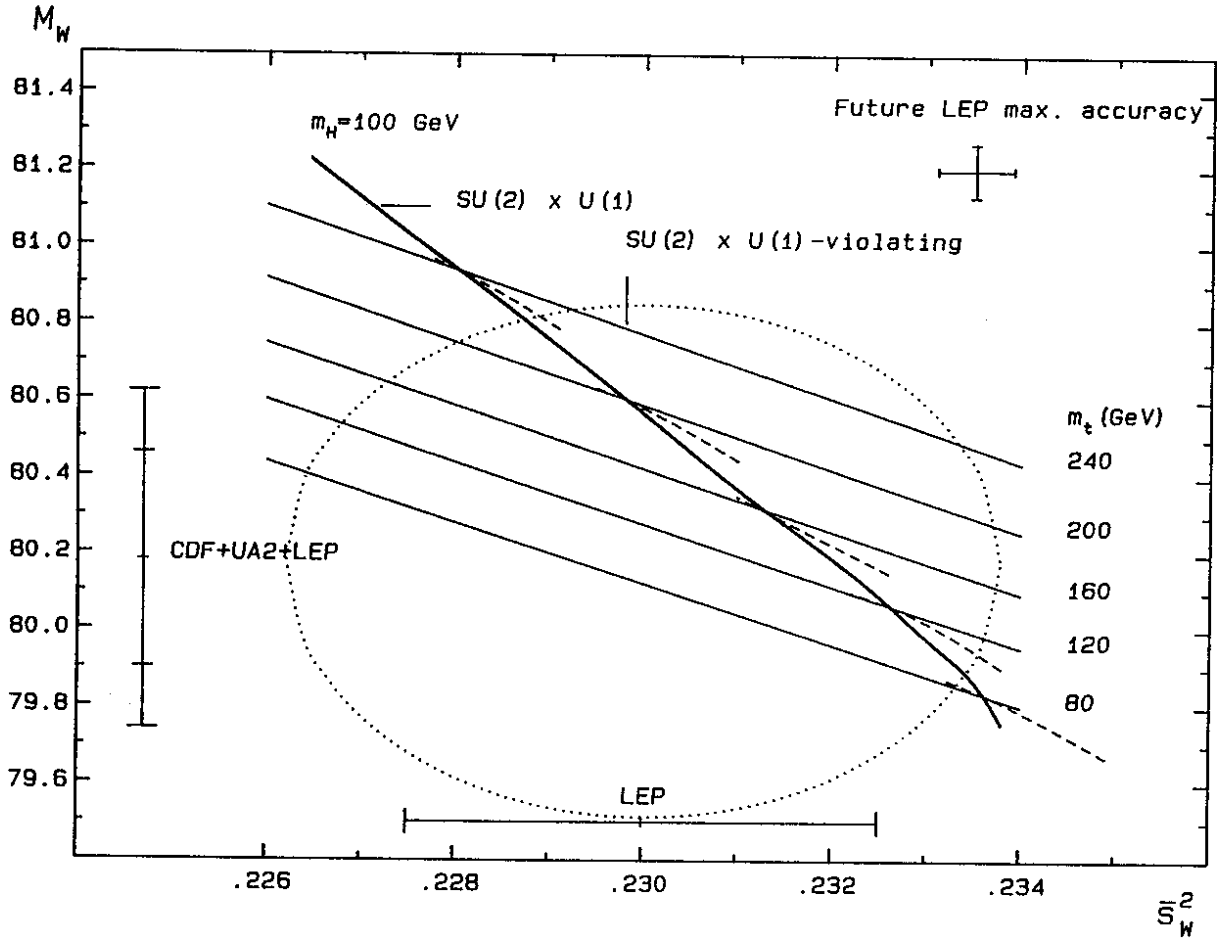

M_W
81.4
81.2
81.0
80.8
80.6
80.4
80.2
80.0
79.8
79.6
m_H=100 GeV
Future LEP max. accuracy
SU(2) x U(1)
SU(2) x U(1)-violating
m_t (GeV)
240
200
160
120
80
CDF+UA2+LEP
LEP
.226
.228
.230
.232
.234
$\bar{s}_W^2$

Fig. 3a

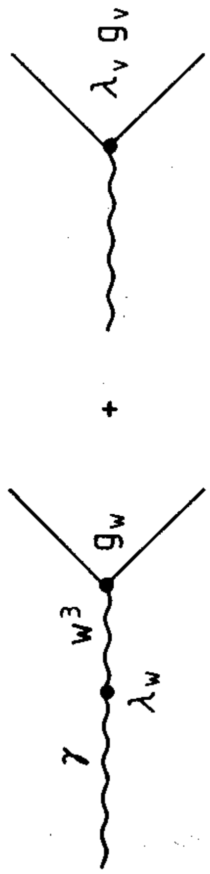

$\lambda_v \; g_v$
+
g_w
W^3
λ_w
γ

Fig. 2

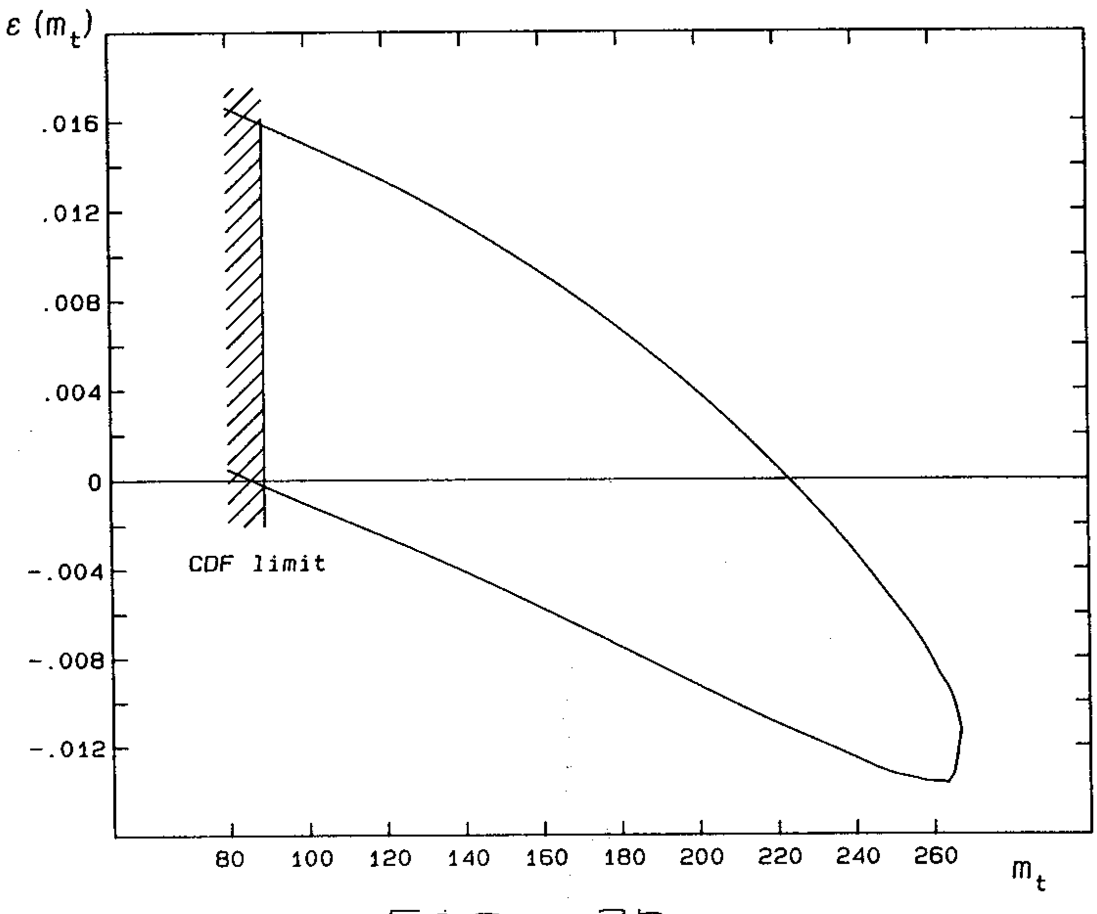

Fig. 3b

Imprimé au CERN. Prix : 0.30 Fr.